Performance Evaluation of Integrated GPS/GIOVE Precise Point Positioning

Wei Cao[1], André Hauschild[2], Peter Steigenberger[3], Richard B. Langley[1], Landon Urquhart[1], Marcelo Santos[1], and Oliver Montenbruck[2]

[(1)]Geodetic Research Laboratory
Department of Geodesy and Geomatics Engineering
University of New Brunswick
Fredericton, N.B., Canada

[(2)]German Space Operations Center
Deutsches Zentrum für Luft- und Raumfahrt
Oberpfaffenhofen, Germany

[(3)]Institut für Astronomische und Physikalische Geodäsie
Technische Universität München
München, Germany

BIOGRAPHIES

Wei Cao is a Ph.D. student in the Department of Geodesy and Geomatics Engineering at the University of New Brunswick (UNB). He obtained his Bachelor’s degree in Geomatics Engineering from Wuhan University, China, in 2004 and his M.Sc. degree in Geomatics Engineering from the University of Calgary, Canada, in 2009. His current research interests are GNSS precise positioning techniques and their applications.

André Hauschild is a Ph.D. candidate at Deutsches Zentrum für Luft- und Raumfahrt’s (DLR’s) German Space Operations Center (GSOC). His research focuses on the estimation of GNSS satellite clocks in real-time. He received his diploma degree in mechanical engineering from the Technical University at Braunschweig, Germany, in March 2007.

Peter Steigenberger is a research assistant at the Institut für Astronomische und Physikalische Geodäsie (IAPG) of Technische Universität München (TUM), Germany. He received his Ph. D. in geodesy from TUM. His major research topic is global GNSS solutions.

Richard B. Langley is a professor in the Department of Geodesy and Geomatics Engineering at UNB, where he has been teaching and conducting research since 1981. He has a B.Sc. in applied physics from the University of Waterloo and a Ph.D. in experimental space science from York University, Toronto. Prof. Langley has been active in the development of GPS error models since the early 1980s and has been a contributing editor and columnist for *GPS World* magazine since its inception. He is a fellow of the International Association of Geodesy, The Institute of Navigation (ION), and the Royal Institute of Navigation. He was a co-recipient of the ION Burka Award for 2003 and received the ION Johannes Kepler Award in 2007.

Landon Urquhart is an M.Sc.E. student in the Department of Geodesy and Geomatics Engineering at UNB where his supervisor is Dr. Marcelo Santos. He received his undergraduate degree from UNB and his main research interests include PPP and neutral atmospheric delay modeling.

Marcelo Santos is a professor in the Department of Geodesy and Geomatics Engineering at UNB. He holds an M.Sc. in geophysics from the National Observatory in Rio de Janeiro, and a Ph.D. in geodesy from UNB. He has been involved in research in the fields of space and physical geodesy, GNSS, and navigation. Dr. Santos is the president of the Geodesy Section of the Canadian Geophysical Union and president of the International Association of Geodesy Sub-Commission 4.3 on remote sensing and modeling of the atmosphere.

Oliver Montenbruck is head of the GNSS Technology and Navigation Group at DLR’s German Space Operations Center. His current research focuses on spaceborne GPS applications and the utilization of new GNSS signals.

ABSTRACT

This paper presents first results for dual-constellation single point positioning (SPP) and precise point positioning (PPP) with GPS and GIOVE. For the first time, a real-time orbit and clock product for GIOVE has been used for positioning, which is based on observations

from the recently established CONGO network. An integrated GPS/GIOVE PPP concept is introduced in this paper and numerical results of GPS/GIOVE positioning solutions in both SPP and PPP modes were obtained. Kinematic data has been collected in a field test with a car-mounted antenna. Additionally, static measurements have been collected with a roof-top antenna.

For SPP, the inclusion of a single GIOVE satellite does not yield significant improvements in the solution for the static measurements. But inclusion of a GIOVE satellite has the beneficial effect of enabling more position solutions, improving positioning continuity for the kinematic observations. For PPP, the inclusion of the GIOVE observations degrades the PPP performance when real-time GIOVE clocks from the Real-Time Clock Estimation (RETICLE) system are used, while the addition of GIOVE observations indeed improves the positioning results when post-processed GIOVE orbits and clocks are used. For the kinematic observations, there are significant improvements in the availability of PPP solutions when adding GIOVE observations in both tests in difficult kinematic environments.

INTRODUCTION

GPS precise point positioning (PPP) has become possible with the availability of precise satellite orbits and clock corrections from the International GNSS Service (IGS) (Dow et al., 2009) and several other organizations. Unlike the traditional differential GPS positioning techniques, e.g. real-time kinematic (RTK), which uses differenced pseudorange (code) and carrier-phase observations between the rover and reference stations, PPP is a standalone precise geodetic positioning method, which uses un-differenced code and phase measurements from a single GPS receiver. Because it does not require a base station when operating in the field and it can be set up in a cost-effective way, PPP has been drawing more and more attention from researchers all over the world. With processing of dual-frequency measurements from a single GPS receiver, position solutions with decimetre- or even centimetre-level accuracies can be obtained in both static and kinematic modes on the global scale. Previously, such accuracy levels could only be achieved through a differential positioning method with processing observations from two or more receivers simultaneously.

The PPP technique has been extensively investigated during the past decade. It was first introduced by Zumberge et al. (1997) at the Jet Propulsion Laboratory (JPL) to reduce the computational burden of processing a large IGS network with hundreds of stations, though originally it was not planned to be used for site positioning. To reduce the convergence time and improve the positioning accuracy, studies have been conducted on adding observations from other GNSS systems, e.g. GLONASS or Galileo, to the current GPS PPP solutions. A combined constellation significantly increases the number of visible satellites and thus improves the geometry of observed satellites, which lead to improvements in PPP availability, reliability, and accuracy. A combined GPS/GLONASS PPP system was developed and demonstrated by Cai and Gao (2007) and Cai (2009), which showed a significant improvement in the position accuracy as well as convergence time compared to the GPS-only PPP: the improvement ratios of the positioning accuracy were 40%, 28% and 24% and the improvement ratios of the convergence time were 21%, 24% and 19% in the east, north and up components, respectively, for six globally distributed IGS stations. Kinematic tests showed that the positioning accuracy had improvements of more than 50% and 30% on horizontal and vertical components, respectively. A commercial service of real-time GPS/GLONASS PPP has been successfully established by the SeaSTAR and OmniSTAR services of Fugro N.V. and has shown superior performance to the GPS-only PPP solutions (Melgard et al., 2009). In addition, Shen and Gao (2006) studied the performance of a combined GPS/Galileo PPP and showed it had significant improvement (up to 75%) on positioning accuracy when compared with the GPS-only solutions with a standard constellation of 24 GPS satellites based on observation simulations. Furthermore, multi-constellation PPP, namely a combined GPS/GLONASS/Galileo PPP, was simulated by Kjørsvik et al. (2007) for hydrographic survey applications. However, these studies were based on computer-simulated observations and might not reflect actual multi-GNSS PPP solutions.

The Galileo experimental satellites, GIOVE-A and -B, were launched in 2006 and 2008, respectively. They are currently transmitting navigation signals on three frequency bands: E1, E5, and E6; however, each satellite only transmits two signals simultaneously, either E1 and E5 or E1 and E6. The status of the signal transmission can be found on the ESA GIOVE website (ESA, 2010). They open opportunities to look into combined GPS/Galileo PPP with real collected data. The COoperative Network for GIOVE Observation (CONGO) has been established by the German Aerospace Center (Deutsches Zentrum für Luft- und Raumfahrt or DLR) and the Federal Agency for Cartography and Geodesy (Bundesamt für Kartographie und Geodäsie or BKG). Data from this network provides precise GIOVE orbit and clock information for scientific research purposes. The University of New Brunswick (UNB) and DLR are collaborating on assessing PPP performance using these products combined with analogous GPS products. An existing GPS PPP software package, GPS Analysis and Positioning Software or GAPS (Leandro, 2009) developed at UNB has been upgraded to handle observations from both GPS and GIOVE satellites. Both static and kinematic data sets have been collected to evaluate the performance of GPS/GIOVE PPP solutions. PPP solutions from GPS alone and GPS/GIOVE have been compared and analyzed in the position domain.

This paper aims at assessing the performance of GPS/GIOVE PPP by using real dual-constellation measurements. For the sake of comparison and completeness, the pseudorange-based single-point-positioning (SPP) performance with GPS/GIOVE observations has also been analyzed. The following section, "Satellite Orbit and Clock Products" describes the generation of precise GPS and GIOVE satellite orbit and clock products used in the data processing. Following a description of the measurement campaigns and test cases, the "Single Point Positioning with GPS and GIOVE" section shows the results of GPS/GIOVE stand-alone positioning using pseudorange measurements. This is followed by the "Precise Point Positioning with GPS and GIOVE" section, which includes the details of data processing of GPS/GIOVE observations for precise-point-positioning purposes and the results of GPS/GIOVE PPP solutions. The "Conclusion" section summarizes the results, draws conclusions, and proposes future research.

SATELLITE ORBIT AND CLOCK PRODUCTS

The positioning results for this paper have been produced using a dedicated orbit- and clock-product, which contains ephemerides for GPS as well as GIOVE satellites. The following sections introduce the origin of this product, starting with the network used to compute the orbits and clock-offset parameters for GIOVE. Afterwards, the orbit determination algorithm and the real-time clock-offset estimation process will be described.

GIOVE Observation Network

The COoperative Network for GIOVE Observation (CONGO) was initiated by DLR/GSOC in January 2008 with the setup of a Septentrio GeNeRx receiver in Sydney, Australia. During 2008 and 2009, additional stations around the world have been set up in a joint effort by DLR and BKG. In July 2009, global coverage of the GIOVE satellites was possible for the first time with CONGO. The state of the network in September 2009 is depicted in Figure 1. At that time, 8 sites were operational and provided measurements for orbit and clock determination of the GIOVE satellites. The station at Stanford became operational in December 2009 and O'Higgins in January 2010.

The stations in Sydney, Concepcion (Chile), and Wettzell (Germany) are equipped with Septentrio's GeNeRx receivers. This type of receiver is also used in ESA's GIOVE tracking network and offers a broad range of GIOVE tracking capabilities. Six user-configurable channels can be used to track GIOVE-A and -B. The receiver supports tracking of signals on the E1, E5a, E5b, and E6 frequencies. Additionally, the combined E5 signal (AltBOC) can be tracked for one satellite. Furthermore, the receiver has channels for up to 9 GPS satellites and reports C/A-, P1-, and P2-observations. In the CONGO network, all GeNeRx receivers are configured to track GIOVE signals on the E1, E5a, and E6 frequencies. All remaining stations except for one are equipped with Javad's new Triumph Delta-G2T or -G3T receivers. The former offers tracking of GPS, GIOVE, and SBAS satellites and the latter additionally supports GLONASS. The Triumph receiver tracks on three frequencies, which are L1/E1, L2 and L5/E5a. Finally, the O'Higgins station is equipped with a Leica GRX1200+GNSS receiver, which supports GPS, GLONASS, GIOVE, and SBAS and tracks L1, L2, and L5 for GPS and E1, E5a, and E5b for GIOVE. The combined E5 (AltBOC) signal is supported as well. Three CONGO stations (Stanford, Chofu, and Fredericton) are equipped with Trimble Zephyr Geodetic II antennas. Wettzell and O'Higgins are equipped with a Leica AR25 antenna, which has been upgraded by the manufacturer with an additional insert in the choke-ring to suppress multipath on the L5/E5a-band. This antenna will also be used for all stations that are currently temporarily equipped with Leica AX1203+GNSS antennas.

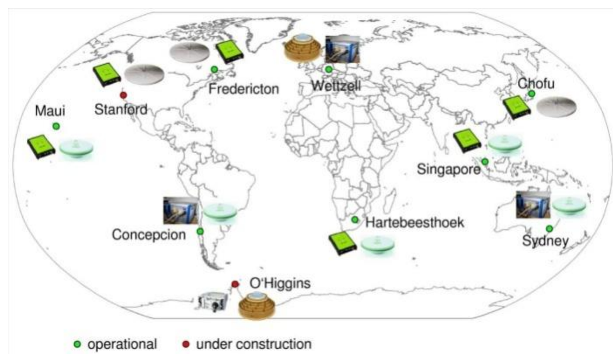

Figure 1: Status of the CONGO Network in September 2009

All stations of the CONGO network transmit their measurements in real-time via the NTRIP protocol to a dedicated caster at BKG (Weber et al., 2005). From there, the streams can be accessed by authorized users and used for real-time processing. The data of the entire network is furthermore recorded and archived at TUM to be used for post-processing. With the current network, the GIOVE satellites are simultaneously tracked by 1 to 4 stations, depending on their orbital position. This depth-of-coverage (DOC) already enables a global orbit and clock determination of the GIOVE satellites as long as they transmit the E1/E5a-frequency combination (Montenbruck et al., 2009).

Orbit and Real-Time Clock Products

The GIOVE orbit predictions provide the basis for the computation of the real-time clocks. The orbit determination and prediction is performed at TUM once a day with a modified version of the Bernese GPS Software 5.0 (Dach et al., 2007). The RINEX files generated from the real-time streams are processed in daily batches. In a first step, station positions, troposphere zenith delays and gradients as well as receiver clock parameters are estimated in a GPS-only PPP mode with the rapid orbit and clock products of the Center for Orbit Determination in Europe (CODE). These GPS-only derived parameters are fixed in the second step and the GIOVE orbit and clock parameters are estimated. The orbit is parameterized by six Keplerian elements and five radiation pressure (RPR) parameters. As code *and* phase observations are used, combined inter-system/inter-frequency biases (ISB) for all stations but one have to be estimated. To get more stable orbit results, a long-arc solution is computed for the orbit predictions. In this multi-day arc, the orbit is represented by one set of orbital elements and RPR parameters thus stabilizing the solution. In the case of CONGO, the normal equations of five consecutive days are combined and the orbit positions are predicted for 2 days to guarantee seamless predictions in the case of latencies in the processing.

Based on the predicted orbits and clocks, a real-time clock-determination system has recently been established at DLR. This system is an extended version of DLR's Real-Time Clock Estimation (RETICLE) system, which has been described by Hauschild and Montenbruck (2008). The extended version combines the measurements of the CONGO network with other GPS real-time data streams to obtain simultaneous estimates of the GPS and GIOVE clock offsets. Since the orbits of the satellites are not part of the estimation, the RETICLE system computes the real-time clocks corresponding to orbit predictions. The Ultra-Rapid predicted orbits (IGU) from the IGS are used for the GPS satellites. The GIOVE orbits stem from daily predictions provided by IAPG/TUM as previously described. Within the RETICLE system, the epochs of orbit and clock information of GIOVE-A and -B refer to GPS System Time to allow for simple use in combined GPS/GIOVE positioning. The GIOVE clocks are modeled in RETICLE's Kalman filter in an identical manner to the GPS clocks with a linear polynomial. Process noise is applied to the clock offset and drift parameters. In addition to the satellite clock offsets and drifts, the Kalman-filter state also comprises the station-clock offsets, the tropospheric zenith delays as well as the float ambiguities of the ionosphere-free combination of the carrier-phase measurements for every satellite tracked by the reference stations.

In accord with established GPS processing conventions, the clock estimates of the GPS constellation are based on the ionosphere-free combination of P1 and P2 observations. For GIOVE, the clock is estimated based on the ionosphere-free combination of the observations on E1 and E5a, since these are the frequencies common to all receivers in the CONGO network. For consistent processing, however, satellite- and receiver-dependent biases of the individual observations must be considered. Eq. 1 is a simplified observation equation for the ionosphere-free pseudorange combination P_{IF} using the frequencies A and B:

$$P_{IF} = \rho + cdT - cdt + b_{rcv,IF(A,B)} + b_{sat,IF(A,B)} + d_{trop} + \varepsilon_{MP,RN} \quad (1)$$

The true range is denoted ρ, the receiver and satellite clock offsets are denoted dT and dt, respectively, and are converted to distance units with the speed of light c. The tropospheric delay is denoted as d_{trop} and $\varepsilon_{MP,RN}$ accounts for the errors due to multipath and receiver noise. $b_{rcv,IF(A,B)}$ denotes a receiver-dependent bias, which consists of the ionosphere-free combination of the absolute biases of the individual frequencies A and B:

$$b_{rcv,IF(A,B)} = \frac{f_A^2}{f_A^2 - f_B^2} b_{rcv,A} + \frac{-f_B^2}{f_A^2 - f_B^2} b_{rcv,B} \quad (2)$$

The corresponding frequencies are denoted f_A and f_B. The same definition holds for the satellite-dependent bias $b_{sat,IF(A,B)}$. As already mentioned before, the clock offsets of RETICLE are estimated to be consistent with the P1/P2-combination, therefore the biases $b_{rcv,IF(P_1,P_2)}$ and $b_{sat,IF(P_1,P_2)}$ are set to zero. The majority of the real-time streams, however, omit the P1 observations in favour of the C/A (or C1) observation. In this case, the ionosphere-free combination is formed from C1/P2. For consistency, the satellite-dependent bias $b_{sat,IF(C_1,P_2)}$ must then be regarded for each satellite. It is formed from the differential code-bias of the C1 and P1 signals and must be scaled with the corresponding factor of the ionosphere-free combination. The receiver-dependent C1/P2-biases are identical for all observations and can therefore be absorbed in the receiver clock offset.

The GIOVE observations are also modeled according to Equation (2). It should be noted, however, that the GIOVE satellite clock offset is estimated with respect to the GPS Time by RETICLE, combining the GPS/GIOVE system time offset (GGTO) and the satellite clock offset into a single estimation parameter. The satellite-dependent bias $b_{sat,IF(E_1,E_{5a})}$ is also merged into the GIOVE clock offset estimate. This simplification ensures that the GIOVE clock offsets are referred to GPS Time and thus spares the user from having to apply these corrections individually. The receiver-dependent biases $b_{rcv,IF(E_1,E_{5a})}$ of the E1E5a-combination must be applied, however, since the receiver clock is consistent with the P1P2- or C1P2-combination, respectively. This bias must be estimated for each CONGO-station and applied during the modeling of the pseudorange observations. It is also referred to as a combined inter-signal- and inter-system-bias (ISB). To avoid an underdetermined system, the bias of the station UNBD is fixed to zero and all other ISBs are estimated relative to UNBD. The RETICLE system uses the CONGO station biases estimated by Bernese at TUM, which are updated once per day. Users of the RETICLE products must also determine the bias of their receiver in order to be able to perform combined GPS/GIOVE-positioning. This can be accomplished for example by determining the position from a GPS-only solution and then averaging the residuals in the GIOVE-observations, which have been computed with RETICLE orbits and clocks.

The RETICLE products are made accessible to users in two different ways: Users with real-time requirements can access NTRIP-streams with the orbit and clock information. For near real-time and offline applications, recorded SP3-files with the GPS and GIOVE orbits and clocks can also be retrieved via FTP. For the analyses in this paper, the latter approach has been used.

STATIC AND KINEMATIC TEST CASES

Two test cases are evaluated in the analysis section of the paper. The first test is a static test with a roof-top antenna. The receiver is a Javad Delta-TRE_G3TH connected to a Trimble Zephyr Geodetic II antenna. The antenna is mounted on the roof of GSOC at the DLR site in Oberpfaffenhofen, Germany. Data has been collected over a 24h period on 14 January 2010 with a data rate of 1 Hz. At that time, GIOVE-A was transmitting on the frequencies E1 and E5 and had extended visibility periods from Oberpfaffenhofen. Since GIOVE-B has been switched to transmit on E1 and E6, which prohibits the orbit and clock estimation with the CONGO network, the analysis is restricted to GIOVE-A only. It should be noted that the receiver used to collect the static measurements is not part of the CONGO network and its data has not been used in the orbit or clock computation. Therefore, the analysis is not affected by the absorption of common errors.

Since the IGU predicted orbits have been used for the GPS satellites, their orbit errors are typically less than 10 cm. The error in the clock-offset estimation for GPS is of the same magnitude. The errors of the GIOVE-A orbit prediction are significantly larger, especially in the along-track direction. The errors summarized in Table 1 have been computed from a comparison with the precise orbit and clock product computed with Bernese at IAPG/TUM. The errors in the real-time GIOVE clocks are also significantly larger compared to GPS, which is due to the effect of the orbit error on the clock estimation as well as the comparably low tracking redundancy of the CONGO network.

Table 1: Mean and standard deviation of GIOVE-A orbit and clock errors for static test (μ: mean, σ: standard deviation, units are meters)

Radial		Tangential		Normal		Clock Offset	
μ	σ	μ	σ	μ	σ	μ	σ
0.04	0.07	-2.13	0.40	0.09	1.09	-0.37	0.22

The second test is a kinematic test with an antenna mounted on a vehicle. This time, a different Javad Delta-TRE_G3T receiver was used, connected to a Leica AX1203+GNSS antenna. The antenna was attached with a magnetic mount to the roof of the car. The tracking data of the receiver was collected with a data rate of 1 Hz on a laptop for later post-processing. The setup is depicted in Figure 2. The data collection took place on 23 September 2009 in Savannah, Georgia, U.S.A. For the first data-recording run, the car took an inbound route from the Savannah International Trade and Convention Center to downtown Savannah, which started at approximately 21:24 UTC and ended at 21:58 UTC. During the second recording run, the car drove outbound from 22:07 to 22:24 UTC on a partially different route. The routes of both test runs are shown in Figure 3. GIOVE-B was visible at an elevation angle between approximately 58° and 64° throughout the test.

Figure 2: Kinematic test setup

The orbit and clock product used for the kinematic test did not originate from the real-time estimation with RETICLE. It has been produced with an offline version of the clock filter, which emulates real-time processing using recorded RINEX files instead of NTRIP data streams for the observations. However, to ensure that the results truly reflect the quality of a real-time product, predicted GPS and GIOVE orbits have been used and measurements have been processed in forward-only mode without any additional smoothing applied.

Again, the IGU predicted orbits have been used for GPS, which yield orbit errors typically less than 10 centimeters. The GPS clock errors are of the same order of magnitude. The errors for the GIOVE-B orbit and clock shown in Table 2 have again been computed from a comparison with the precise orbit and clock product from Bernese.

Table 2: Mean and standard deviation of GIOVE-B orbit and clock errors for kinematic test (μ : mean, σ : standard deviation, units are meters)

Radial		Tangential		Normal		Clock Offset	
μ	σ	μ	σ	μ	σ	μ	σ
0.24	0.09	4.65	1.10	-0.05	1.24	0.19	0.52

Figure 3: Trajectory for kinematic test showing the inbound route to downtown Savannah (top plot) and the outbound route (bottom plot) (imagery courtesy of Google)

SINGLE POINT POSITIONING WITH GPS AND GIOVE

The measurements of both tests have been processed in a single-point-positioning algorithm. This algorithm makes use of pseudorange measurements only and computes a positioning solution at each single epoch (point) using a least-squares fit. The UNB3-model is used for the tropospheric correction of the modeled pseudorange (Collins et al., 1996). Data editing is performed based on a screening of residuals. If the RMS of the individual pseudorange residuals exceeds a predefined threshold, the position solution and the RMS residual is recomputed with a single satellite rejected. This procedure is recursively repeated with each satellite tracked at this epoch to find the subset-solution which yields the lowest residual. The rejected satellite is then omitted from the navigation solution at this epoch. This data editing procedure can of course only be executed with more than 5 satellites. If the number of satellite drops down to five, no positioning solution can be computed in case the RMS threshold is exceeded. For the analysis of this paper, the pseudorange RMS threshold has been set to 5 m.

Static Observations

Prior to being able to process the measurements of the static test with the aforementioned SPP algorithm, the inter-system/inter-frequency bias of the GIOVE-observation for this receiver- and antenna-combination must be determined. This has been done by processing a previous GIOVE-A satellite pass with comparable length using the final orbits and clocks computed with Bernese at IAPG/TUM. The mean of the pseudorange residuals yields an ISB of -1.9 m. The static data has then been processed using the real-time orbit- and clock-product from the RETICLE system. To emphasize differences between both solutions, only the time interval of the GIOVE-A pass was processed, which started at 02:47 UTC and ended at 10:45 UTC. For the SPP processing the observations have been decimated to 10-second intervals. The reference position has been determined with GAPS using the final GPS orbit and clocks from IGS.

The results of the RMS errors of the SPP solution are summarized in Table 3. The comparison to the reference position reveals errors of 0.73 m in the east-direction and 1.05 m in the north-direction. The up-component exhibits the largest error of about 2 m as expected. The mixed GPS/GIOVE positioning shows that the errors are still approximately the same. However, a slight improvement of a few centimeters compared to the GPS-only solution is visible.

Table 3: RMS errors of the single point positioning results for static test using GPS-only processing and combined GPS/GIOVE processing (units are meters)

Constellation	North	East	Up	3D
GPS	1.05	0.73	1.98	2.36
GPS/GIOVE	0.99	0.71	1.93	2.28

Kinematic Observations

For both test runs, a navigation solution has been computed with GPS satellites exclusively as well as using GPS and GIOVE. It should be noted that GIOVE is indeed used in all position solutions except for 4 epochs in the first test and 2 epochs in the second test. The ISB has been determined in a similar way as for the static measurements. The receiver had been connected to a roof-top antenna, which is of the same model as the antenna used in the kinematic test. The inter-system bias amounts to 1.0 m in this case. Note that since different equipment has been used for the two measurement campaigns, the ISB is different for both cases.

For the first test run, a total of 2035 epochs have been recorded. The SPP algorithm is able to compute in total 1742 valid position solutions. The positioning fails for the remaining epochs, since the number of valid pseudorange observations drops below 6. On the one hand, this is due to signal blocking especially in the downtown area of Savannah. On the other hand, the data-editing algorithm rejects degraded measurements at certain epochs, until the number of valid observations falls below the required minimum. The inclusion of GIOVE-B makes a significant difference here. The number of valid positions increases to 1906 for this test run. The difference in the availability of the navigation solution for downtown Savannah is depicted in Figure 4 and Figure 5. The second test run yields comparable results. In total, 963 epochs were recorded in this test. Positioning with GPS only yields 893 position solutions, whereas GPS and GIOVE together increase this number to 936.

Figure 4: Position solutions in downtown Savannah from single point positioning with GPS+GIOVE (imagery courtesy of Google)

Figure 5: Position solutions in downtown Savannah from single point positioning with GPS only (imagery courtesy of Google)

Table 4: Number of valid epochs of SPP solutions for kinematic tests

	Test 1		Test 2	
	GPS	**GPS/GIOVE**	**GPS**	**GPS/GIOVE**
No. of Epochs	1742	1906	893	936

PRECISE POINT POSITIONING WITH GPS AND GIOVE

PPP Software - GAPS

GAPS is a software package developed for positioning and GPS data analysis at the University of New Brunswick. One of the main purposes of the development is to use it as a powerful positioning tool, though it has also been used as a versatile tool for GPS data analysis, such as ionospheric and tropospheric delay estimation, differential code biases estimation and code multipath and noise analysis (Leandro et al., 2007). The standard PPP observation model using dual-frequency code and phase ionosphere-free combinations is adopted in GAPS, and it is briefly described as follows,

$$P_i = \rho + cdT - cdt + d_{orb} + d_{trop} + d_{ion/P_i} + d_{mult/P_i} + \varepsilon_{P_i} \quad (3)$$

$$\Phi_i = \rho + cdT - cdt + d_{orb} + d_{trop} - d_{ion/\Phi_i} + \lambda_i N_i + d_{mult/\Phi_i} + \varepsilon_{\Phi_i} \quad (4)$$

where

P_i is the measured pseudorange on L_i (m)
Φ_i is the measured carrier phase on L_i (m)
ρ is the true geometric range (m)
c is the speed of light (m/s)
dT is the receiver clock error (s)
dt is the satellite clock error (s)
d_{orb} is the satellite orbit error (m)
d_{trop} is the tropospheric delay (m)
d_{ion/L_i} is the ionospheric delay on L_i (m)
λ_i is the wavelength of L_i (m/cycle);
N_i is the phase ambiguity parameter on L_i (cycle);
d_{mult/P_i} is the pseudorange multipath effect on L_i (m)
d_{mult/Φ_i} is the carrier phase multipath effect on L_i (m)
ε_{P_i} is the pseudorange measurement noise on L_i (m)
ε_{Φ_i} is the carrier phase measurement noise on L_i (m)

The ionosphere-free linear combination for the pseudorange and carrier-phase measurements can be found from:

$$P_{IF} = \frac{f_1^2 \cdot P_1 - f_2^2 \cdot P_2}{f_1^2 - f_2^2} = \rho + cdT - cdt + d_{trop} + d_{mult/P_{IF}} + \varepsilon_{P_{IF}} \quad (5)$$

$$\Phi_{IF} = \frac{f_1^2 \cdot \Phi_1 - f_2^2 \cdot \Phi_2}{f_1^2 - f_2^2} = \rho + cdT - cdt + d_{trop} + \lambda_{IF} N_{IF} + d_{mult/\Phi_{IF}} + \varepsilon_{\Phi_{IF}} \quad (6)$$

where

P_{IF} is the ionosphere-free pseudoranges on GPS L_1 and L_2
Φ_{IF} is the ionosphere-free carrier phase on GPS L_1 and L_2
λ_{IF} is the equivalent wavelength of ionosphere-free carrier-phase observations
N_{IF} is the ambiguity parameter of ionosphere-free carrier-phase observations

Equations (5) and (6) show the ionosphere-free code and phase observations on two GPS frequencies – L1 and L2 – after applying orbit and clock corrections from IGS products. The ambiguity parameter N_{IF} is a non-integer value since it is formed from the ionosphere-free combination of the integer ambiguities of the individual frequencies.

The three coordinate components, receiver clock error, neutral zenith tropospheric delay and ambiguity parameter of each satellite are estimated as unknown states in a sequential Least-squares filter. The state updates are computed at every epoch of observation, according to Equation (8).

$$\delta = (A^T P A + C_x^{-1})^{-1} A^T P w \quad (7)$$

where

δ is the state's update vector
A is the design matrix
P is the measurement weight matrix
C_X is the state's covariance matrix
w is the misclosure vector

Details on the least-squares filter are given by Leandro (2009). The corrections of various error budget contributions were also described in detail in this reference.

In order to consistently process the GIOVE observations together with GPS in GAPS, the observations on the E1 and E5a frequency are used for the ionosphere-free linear combinations in Equation (5) and (6) with two modifications: First, the frequency factors must be changed accordingly. Second, the station-dependent ISB $b_{rcv,IF(E_1,E_{5a})}$ must be included in the modeling of the pseudorange observation in Equation (5). Since the CONGO GIOVE satellite orbits and clocks are generated in the same time and geodetic reference frames as GPS, no reference frame transformations or system time transformations are required.

Static Observations

PPP solutions have been computed for the static data using exclusively GPS satellites as well as GPS and GIOVE satellites. The position errors in three direction components are shown in Figure 6 and the number of GPS and GIOVE satellites used in both solutions are shown in Figure 7. The second pass of the GIOVE-A satellite was used in the GPS/GIOVE solution before it dropped down to an elevation angle of 15°. It can be seen from Figure 6, the position errors increase when adding GIOVE observations into the PPP solution. Statistics in Table 5 show that the position RMS errors increase in each direction component, especially in the north and east directions. Figure 8 shows the pseudorange and carrier-phase observation residuals of each satellite for both solutions. It can be seen from the plot that the residuals of the GIOVE observations are larger than the residuals of the GPS observations. The pseudorange residuals are significantly biased. The carrier-phase residuals exhibit large variations over time.

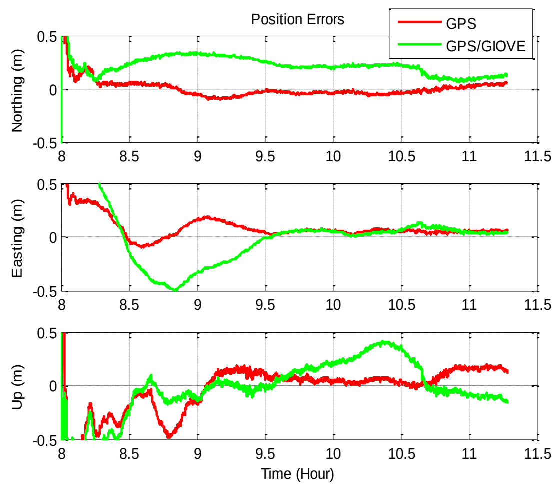

Figure 6: Position errors of PPP solutions for GPS and GPS/GIOVE

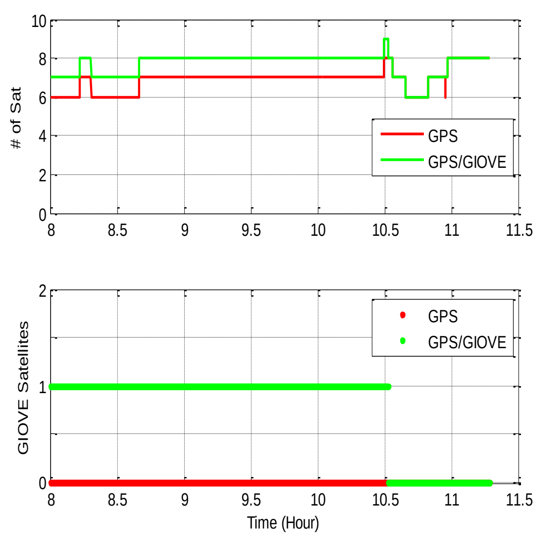

Figure 7: Number of GPS and GIOVE satellites used in the PPP solutions for static test

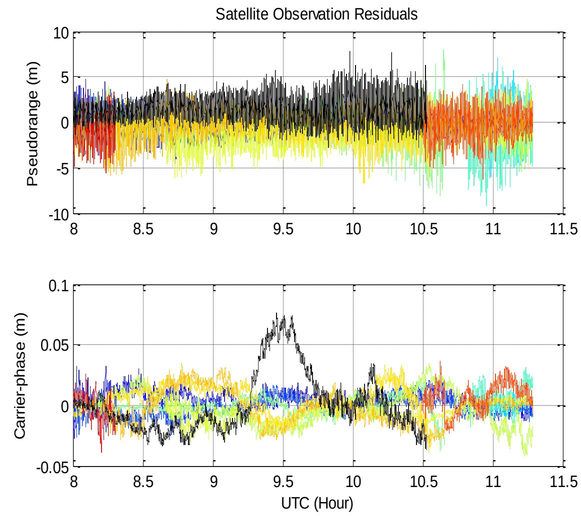

Figure 8: Observation residuals of GIOVE-A (black) and GPS satellites

Table 5: Position error of PPP solutions for static test (units are meters)

Constellation	North	East	Up	3D
GPS	0.045	0.075	0.146	0.170
GPS/GIOVE	0.221	0.156	0.159	0.314

For the processing results depicted in Figures 6 and 8, the GIOVE and GPS observations have been processed with identical data weights. In order to verify that the inclusion of GIOVE observations degraded the PPP positioning performance, the GIOVE observations in the PPP filter were down-weighted stepwise by increasing the *a priori* standard deviation of GIOVE observations by factors of 5, 10, and 20. The PPP solutions with de-weighed GIOVE observations with comparison to GPS-only and the original GPS/GIOVE solutions are shown in Figure 9. It can be seen that smaller position errors are obtained with de-weighted GIOVE observations. When increasing the standard deviation by a factor of 20, the results are nearly identical to the GPS-only solution since the GIOVE observations have a very small effect in the PPP processing. Table 6 summarizes the statistics of position RMS errors of different PPP solutions with de-weighted GIOVE observations. Figures 10-12 show the observation residuals of PPP solutions by de-weighting GIOVE observations. Again, these figures show there are large errors in modeling the GIOVE carrier-phase observations with a maximum of 20 centimeters when increasing the standard deviation of GIOVE observations by a factor of 10 and 20. It is suspected that the mismodeling is due to errors in the real-time GIOVE clock estimates as discussed later. These errors are absorbed into the position solution, leading to biased coordinate estimates when GIOVE observations have the same adjustment weight as those of GPS as shown in Figure 6.

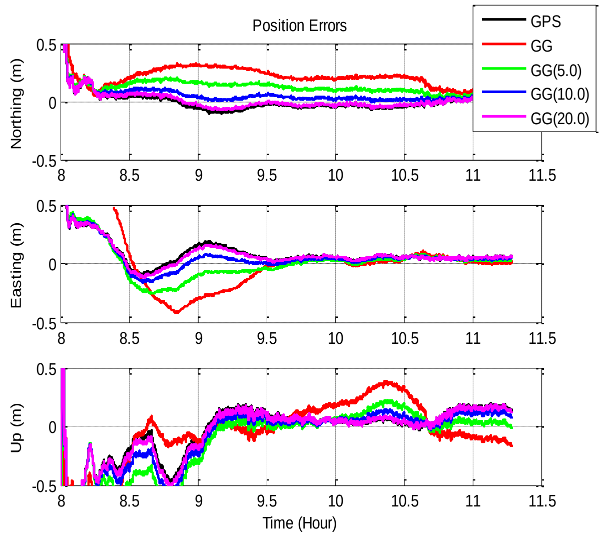

Figure 9: Position errors of PPP solutions with de-weighted GIOVE observations

Table 6: Position errors of PPP solutions with de-weighted GIOVE observations (units are meters)

Increase of Obs. Std. (times)	North	East	Up	3D
1	0.221	0.156	0.159	0.314
5	0.123	0.095	0.218	0.168
10	0.047	0.057	0.177	0.192
20	0.038	0.069	0.155	0.174

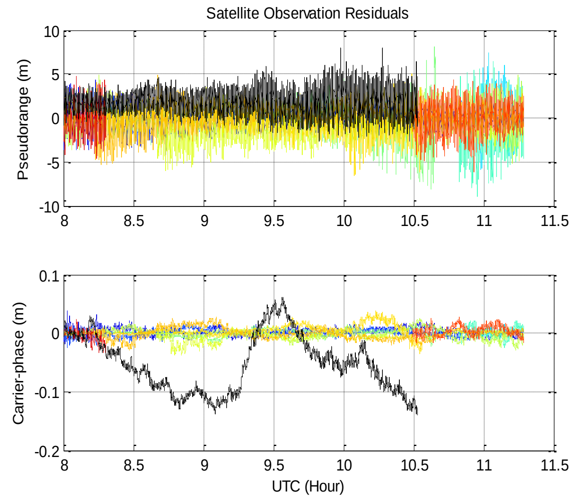

Figure 10: Observation residuals of GIOVE (black) and GPS satellites with increasing the standard deviation of GIOVE observations by a factor of 5

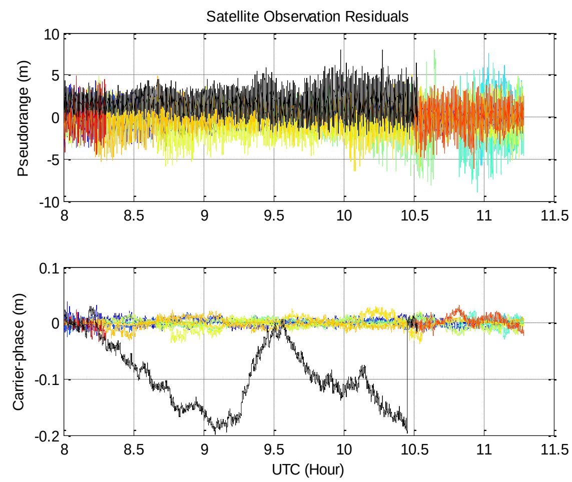

Figure 11: Observation residuals of GIOVE (black) and GPS satellites with increasing the standard deviation of GIOVE observations by a factor of 10

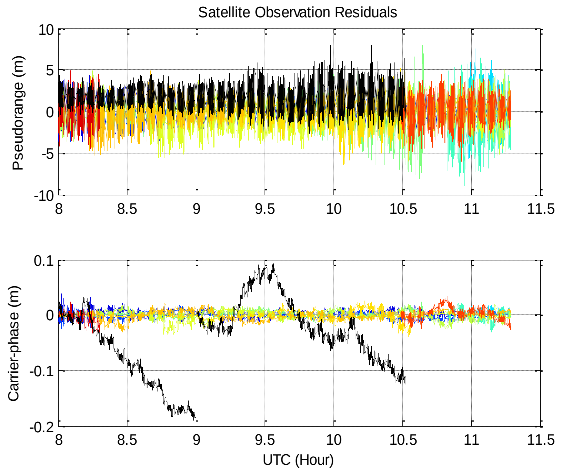

Figure 12: Observation residuals of GIOVE (black) and GPS satellites with increasing the standard deviation of GIOVE observations by a factor of 20

In addition to the PPP solutions with real-time orbits and clocks, GPS-only and GPS/GIOVE solutions were generated using post-processed orbits and clocks. For GPS, the rapid orbit and clock products from CODE have been used. For GIOVE, the middle-day of the post-processed 5-day solution from TUM has been used. Figure 13 shows the position errors for both solutions. The RMS errors of both solutions are given in Table 7, which indicate that the addition of GIOVE observations improves the GPS PPP solution when final GIOVE clocks are used.

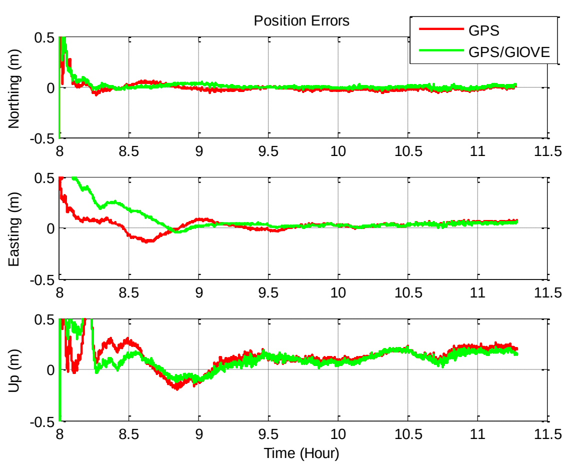

Figure 13: Position errors of PPP solutions for GPS with rapid CODE products and for GPS/GIOVE with final GIOVE clocks from Bernese software

Table 7: Position errors of PPP solutions with post-processed orbits and clocks (units are meters)

Constellation	North	East	Up	3D
GPS	0.027	0.050	0.144	0.155
GPS/GIOVE	0.014	0.048	0.120	0.130

Kinematic Observations

For both kinematic test runs, PPP solutions were computed with GPS satellites and GPS satellites together with GIOVE-B. The emulated real-time orbit and clock products for GPS and GIOVE have been used in the processing. Figure 14 shows the two solutions in the area of downtown Savannah, where the sky view was partially blocked by buildings and trees. It can be seen that the integrated GPS/GIOVE solution significantly improves the availability of PPP solutions. Note that there is a requirement of a minimum of five satellites to obtain a PPP solution as indicated by the black line in Figure 15, which shows the number of GPS and GIOVE satellites used in the solutions. Table 8 summarizes the number of epochs which have PPP solutions available for both test runs. The addition of GIOVE observations makes significant improvements in terms of PPP solution availability. For the first test run, the number of valid epochs increases from 1868 to 2001 when GIOVE observations are included. For the second test run, this number increases from 889 to 939. The increase is still significant considering that only 963 epochs of data were recorded.

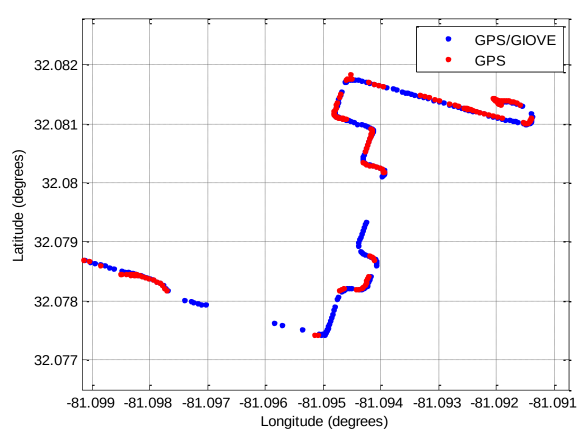

Figure 14: Position solutions in downtown Savannah from PPP with GPS and GPS/GIOVE

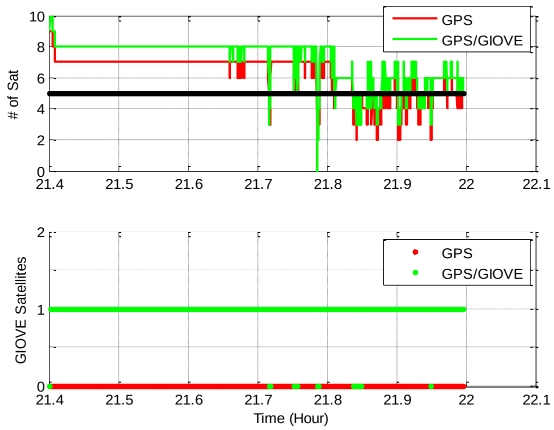

Figure 15: Number of GPS and GIOVE satellites used in the PPP solutions for kinematic test 1

Table 8: Number of valid epochs of PPP solutions for kinematic tests

	Test 1		**Test 2**	
	GPS	GPS/GIOVE	GPS	GPS/GIOVE
No. of Epochs	1868	2001	889	939

CONCLUSIONS AND FUTURE WORK

In this paper, first positioning results using real-time orbit and clock products for the GIOVE satellites have been presented. These products have been generated based on observations from CONGO, a real-time-capable network dedicated to GIOVE observation. The integrated GPS/GIOVE PPP concept has been introduced in this paper. Data sets from a kinematic and a static measurement campaign have been processed with single point positioning and precise point positioning techniques.

For single point positioning, the inclusion of the GIOVE satellite yields marginal improvements in the solution for the static measurements. For a rooftop antenna with nearly un-obstructed sky visibility, a sufficient number of GPS satellites can be tracked to compute a sound positioning solution. Thus, the addition of a single satellite does not have a high impact on the results. The kinematic measurements have been recorded in a challenging environment with significant signal blocking and high multipath errors. The inclusion of the GIOVE satellite has the beneficial effect of enabling more position solutions, improving positioning continuity. The effects on the positioning accuracy could not be assessed in this case for lack of a reference or "truth" trajectory.

For precise point positioning, the inclusion of the GIOVE observations degrades the PPP performance when real-time GIOVE clocks from the RETICLE systems are used, which is due to the fact that the accuracy of GIOVE clocks is lower than those of GPS satellites. A reduced accuracy of the GIOVE real-time product could be expected, since the CONGO network is significantly smaller than the real-time network used for GPS. Future investigations will be directed towards the improvement of the GIOVE real-time clock estimation.

However, the addition of GIOVE observations indeed improves the positioning results when final post-processed GIOVE clocks from TUM are used. For the kinematic observations in a challenging urban environment, there are significant improvements in the availability of PPP solutions when adding GIOVE observations.

The calculation of RMS error statistics for the kinematic measurements was not possible since no precise reference trajectory was available. The latter can be generated with respect to a reference station using carrier-phase-based differential GPS. This will be considered for future field experiments, where more data in both static and kinematic modes in different locations will be collected to further assess the performance of GPS/GIOVE PPP.

ACKNOWLEDGEMENTS

The work described in this paper was supported by the Natural Sciences and Engineering Research Council of Canada. We thank Rodrigo Leandro for helpful advice on PPP processing.

REFERENCES

Cai C. (2009). *Precise Point Positioning Using Dual-Frequency GPS and GLONASS Measurements*. UCGE Report Number 20291, Department of Geomatics Engineering, University of Calgary, Calgary, Canada, August 2009.

Cai C. and Y. Gao. (2007). "Precise Point Positioning Using Combined GPS and GLONASS Observations." *Journal of Global Positioning Systems*, Vol. 6, No. 1, pp. 13-22.

Collins P., R. Langley, and J. LaMance. (1996). "Limiting Factors in Tropospheric Propagation Delay Error Modelling for GPS Airborne Navigation." In *Proceedings of The Institute of Navigation 52nd Annual Meeting*, 19-21 June 1996, Cambridge, Massachusetts, pp. 519-528.

Dach R., U. Hugentobler, P. Fridez, and M. Meindl. (2007). *Bernese GPS Software Version 5.0*, Astronomical Institute, University of Bern, Bern, Switzerland.

Dow, J.; Neilan, R. & Rizos, C. The International GNSS Service in a changing landscape of Global Navigation Satellite Systems Journal of Geodesy, 2009, Vol. 83, No. 3-4, pp. 191-198.

ESA (2010). GIOVE Signal Transmission, published online, URL: http://www.giove.esa.int, last accessed Feb. 2010.

Hauschild A. and O. Montenbruck (2008) "Real-time Clock Estimation for Precise Orbit Determination of LEO-Satellites." In *Proceedings of ION GNSS 2008*, the 21st International Technical Meeting of the Satellite Division of The Institute of Navigation, 16-19 September 2008, Savannah, Georgia, pp. 581-589.

Kjørsvik N.S., O. Øvstedal, and J.G.O. Gjevestad. (2009). "Kinematic Precise Point Positioning During Marginal Satellite Availability." In *Observing our Changing Earth*, Proceedings of the 2007 IAG General Assembly, Perugia, Italy, 2-13 July 2007, M.G. Sideris, editor, Springer Verlag, Symposia Series, Vol. 133, pp. 691-699.

Kouba, J. and P. Héroux. (2001). "Precise Point Positioning Using IGS Orbit and Clock Products." *GPS Solutions*, Vol. 5, No. 2, pp. 12–28.

Leandro, R.F. (2009). *Precise Point Positioning with GPS: A New Approach for Positioning, Atmospheric Studies, and Signal Analysis.* Ph.D. dissertation, Department of Geodesy and Geomatics Engineering, Technical Report No. 267, University of New Brunswick, Fredericton, New Brunswick, Canada, 232 pp.

Leandro, R.F., M.C. Santos, and R.B. Langley (2007). "GAPS: The GPS Analysis and Positioning Software - A Brief Overview." In *Proceedings of ION GNSS 2007*, the 20th International Technical Meeting of the Satellite Division of The Institute of Navigation, Fort Worth, Texas, 25-28 September 2007, pp. 1807-1811.

Melgard T., E. Vigen, K. de Jong, D. Lapucha, H. Visser and O. Oerpen (2009). "G2 - The First Real-Time GPS and GLONASS Precise Orbit and Clock Service." In *Proceedings of ION GNSS 2009*, the 22nd International Meeting of the Satellite Division of The Institute of Navigation, Savannah, GA, 22-25 September 2009, pp. 1885-1891.

Montenbruck O., A. Hauschild, U. Hessels, P. Steigenberger, and U. Hugentobler. (2009). "CONGO - First GPS/GIOVE Tracking Network for Science, Research." *GPS World*, Vol. 20, No. 9, September 2009, pp. 36-41.

Shen X. and Y. Gao. (2006). "GPS/Galileo PPP, Analyzing the Impacts of Galileo and Modernized GPS on Precise Point Positionin.", In *Proceedings of the Institute of Navigation National Technical Meeting 2006*, 18-20 January 2006, Monterey, California, pp. 837-846.

Weber G., D. Dettmering, and H. Gebhard. (2005). "Networked Transport of RTCM via Internet Protocol (NTRIP)." In *A Window on the Future of Geodesy*, Proceedings of the IAG General Assembly, Sapporo, Japan, 2003, F. Sanso, editor, Springer Verlag, Symposia Series, Vol. 128, pp. 60-64.

Zumberge, J.F., M.B. Heflin, D.C. Jefferson, M.M. Watkins, and F.H. Webb (1997). "Precise Point Positioning for the Efficient and Robust Analysis of GPS Data from Large Networks." *Journal of Geophysical Research*, Vol. 102, No. B3, pp. 5005–5018.